IJAME

Int. J. of Applied Mechanics and Engineering, 2026, vol.32, No.2, pp.31-49
DOI: 10.59441/ijame/218522

PROGNOSTIC ASSESSMENT OF SYMMETRIC PERPENDICULAR EDGE CRACKS ON THE VIBRATION CHARACTERISTICS OF ORTHOTROPIC CANTILEVER COMPOSITE PLATES

I.J. Hasan[1*] and T.T. Othman[2]
[1]Power Mechanics Technics, Northern Technical University, IRAQ
[2]Petroleum Control Systems Engineering, College of Petroleum Processes Engineering, Tikrit University, IRAQ
E-mail: iesam.j.hasan@ntu.edu.iq

This study investigates the free vibration characteristics of orthotropic cantilever composite plate containing symmetric double edge cracks. A detailed finite element analysis (FEA) was conducted in ANSYS APDL to investigate the influence of crack length $\left(\frac{a}{W}=0.04\right)$ and crack location $\left(\frac{x_c}{L}=0-0.75\right)$ on the first six natural frequencies. The results show a consistent frequency reduction with increasing crack length and proximity to the clamped edge, while higher-order modes display greater sensitivity due to localized strain energy near the cracks. A semi-empirical relation was also developed to predict frequency degradation based on crack geometry and position, achieving excellent agreement with numerical data $\left(R^2>0.99\right)$. The findings provide a concise framework for vibration-based damage detection and structural health monitoring (SHM) of orthotropic composite structures. Unlike previous works that primarily examined single-edge or isotropic configurations, this study uniquely quantifies the coupled influence of symmetric double-edge cracks in orthotropic cantilever plates, thereby extending the understanding of multi-crack interaction effects in composite dynamics.

Key words: orthotropic composite, edge cracks, cantilever plates, modal analysis, natural frequencies.

1. Introduction

Composite structures, particularly those composed of orthotropic materials, have become increasingly prevalent in advanced engineering applications due to their superior strength-to-weight ratio, tailored stiffness properties, and resistance to environmental degradation. These attributes have made orthotropic composite plates indispensable in aerospace, automotive, marine, and civil infrastructure systems, where dynamic loading conditions and structural reliability are of critical concern. Among the many design configurations, cantilever plates are especially significant due to their common use in sensor platforms, turbine blades, robotic arms, and structural appendages.

However, despite their mechanical advantages, composite plates remain vulnerable to damage in service, most notably in the form of cracks. Edge cracks, especially when symmetrically positioned, represent a severe form of structural discontinuity that can significantly alter the stiffness distribution, degrade the vibrational performance, and ultimately compromise the structural integrity. Since many of these systems operate under dynamic conditions, the alteration of their natural frequencies and mode shapes due to cracking can serve as both a symptom of damage and a source of failure if undetected. While numerous studies have examined single crack effects in isotropic and composite plates, the impact of *double symmetric edge cracks* in *orthotropic cantilever configurations* remains insufficiently addressed. This lack of comprehensive

* To whom correspondence should be addressed

understanding limits the development of effective vibration-based diagnostic and prognostic tools tailored for orthotropic composite structures, particularly those with complex damage configurations.

Extending the operational life of composite or metallic structural systems under harsh environmental conditions has become a major research focus due to increasing need for cost-effective and sustainable designs. Recent comprehensive reviews on offshore support structures emphasized the importance of advanced monitoring systems, material durability, and structural reinforcement methods to enhance longevity (Zavvar *et al.* [1]).

Research on the dynamic response of cracked structural members has gained significant momentum, especially for composite and orthotropic materials frequently employed in aerospace, civil, and mechanical engineering systems. Foundational analytical developments, such as those reported by Natarjan *et al.* [2] and Tran *et al.* [3], utilized extended finite element and isogeometric frameworks to model cracked and functionally graded laminated plates, emphasizing how crack geometry modifies both fundamental and higher-order mode frequencies. Building upon these developments, Wu *et al.* [4] implemented a modified two-dimensional Fourier Series Method to study orthotropic plate vibration, achieving enhanced convergence and accuracy across multiple modes. In a related effort, Zhang *et al.* [5] delivered analytical solutions for orthotropic plates with partial edge restrains, demonstrating the influence of restraint conditions on mode coupling and frequency attenuation.

A combination of numerical and experimental contributions has also enriched the understanding of crack-vibration interactions. Rezaee *et al.* [6] applied a disturbance function-based approach to predict frequency degradation in cracked beams, whereas Shehab *et al.* [7] compared intact and cracked functionally graded plates, concluding that cracks aligned with high strain energy regions cause the most pronounced dynamic deterioration. Hu *et al.* [8] developed a symplectic superposition method for in-plane vibration of orthotropic plates and confirmed its validity through benchmark comparisons. Similarly, Eshete *et al.* [9] combined experimental measurements with simulations on unidirectional and quasi-isotropic plates containing edge cracks, verifying the crack-induced stiffness reduction, particularly for higher vibration modes.

From a computational standpoint, recent progress has enabled more realistic modeling of crack effects in orthotropic components. Zuyev *et al.* [10] integrated analytical formulations with data-driven models to simulate orthotropic plate dynamics, while Guo *et al*. [11] used a numerical manifold method capable of handling cracks with arbitrary orientations. Stress intensity factors and crack opening displacement under anti-plane shear in orthotropic strips were analyzed by Karan *et al.* [12], providing fracture mechanics insights relevant to vibration degradation. Analytical work by Chen *et al.* [13] further demonstrated how variable boundary conditions in cracked rectangular plates effect modal characteristics, reinforcing the necessity of accurate boundary modeling.

Investigations on laminated and microscale plates have expanded this scope. Yang and He, [14] employed modified couple stress theory to assess the vibration of functionally graded orthotropic microplates, while Dwivedi *et al*. [15] combined higher-order shear deformation theory with XFEM for cracked laminated composites under free vibration. Adimass *et al*. [16] supplemented these findings with combined experimental-numerical analysis of hybrid composite beams containing edge cracks, identifying a nonlinear reduction in natural frequencies with increasing crack length and varying orientation.

Practical relevance has been emphasized in several studies. Al-Waily and Al-Shanmmari [17] analyzed dynamic instability in orthotropic hybrid composite plates using theoretical and numerical models, pinpointing crack location as a decisive parameter. Al-Shammari [18] demonstrated through finite element analysis that even shallow cracks can substantially modify dynamic response in composite beams. Brethee [19] employed the AFESPI technique to characterize vibrational behavior of edge-cracked composite plates, while Lai *et al*. [20] explored the combined influence of thermal and mechanical loads on orthotropic cracked plates, providing insights into thermos-vibration coupling.

In this study, a high-fidelity numerical investigation is conducted to evaluate the influence of symmetric double-edge cracks on the modal characteristics of orthotropic cantilever composite plates. While numerous studies have explored vibration degradation caused by single-edge cracks or isotropic materials, systematic investigations addressing double symmetric cracks in orthotropic cantilever configurations remain scarce. This research therefore bridges that gap by quantifying how the combined effects of crack symmetry, orthotropy, and crack positioning influence the dynamic response. The outcomes not only extend previous

single-crack models, nut also establish a predictive framework applicable to multi-cracked orthotropic structures.

2. Theoretical background

Orthotropic composite plates, characterized by directional stiffness, are widely used in engineering applications where weight and strength optimization are critical. When such plates are subjected to damage in the form of double symmetric edge cracks, their dynamic behavior- especially natural frequencies and mode shapes- is significantly affected due to local stiffness degradation. This section presents the theoretical formulation for modeling the vibrational behavior of orthotropic cantilever plates with such defects.

The theoretical framework presented here is not a generic overview but forms the analytical foundation for the numerical modeling carried out in ANSYS APDDL. Each equation was adapted to represent the specific conditions of an orthotropic cantilever composite plate containing symmetric edge cracks. Accordingly, the theoretical formulations serve to establish how crack-induced stiffness degradation is reflected in the vibration characteristics investigated later in the numerical analysis.

2.1. Governing equation of free vibration for orthotropic plates

The present formulation is based on the Classical Plate Theory (CPT), also known as the Kirchhoff-Love theory, which neglects transverse shear deformation effects. This assumption is appropriate for thin orthotropic composite plates where the thickness-to-length ratio (h/L) or (h/W) is less than 0.1. Under such conditions, the influence of shear deformation on the natural frequencies becomes negligible [21, 22].

The free transverse vibration of a thin orthotropic plate is governed by the following partial differential equation (based on classical plate theory) [21-23]:

$$D_x \frac{\partial^4 w}{\partial x^4} + 2H \frac{\partial^4 w}{\partial x^2 \partial y^2} + D_y \frac{\partial^4 w}{\partial y^4} + \rho h \frac{\partial^2 w}{\partial t^2} = 0 \tag{2.1}$$

where:

$w(x,y,t)$: transverse displacement,

$D_x = \dfrac{E_x h^3}{12\left(1 - v_{xy} v_{yx}\right)}$: flexural rigidity in the x-direction,

$D_y = \dfrac{E_y h^3}{12\left(1 - v_{xy} v_{yx}\right)}$: flexural rigidity in the y-direction,

$H = \dfrac{h^3}{12\left(1 - v_{xy} v_{yx}\right)}\left(v_{xy} E_y + v_{yx} E_x\right)$: coupling rigidity,

ρ: material density,

h: plate thickness.

For the present configuration, the governing equation (Eq.2.1) was implemented under cantilever boundary conditions, consistent with the finite element setup described on Section 3. This ensures that the analytical assumptions directly correspond to the simulated model, allowing the theoretical stiffness parameters (D_x, D_y, and H) to guide the definition of orthotropic materials behavior in ANSYS.

In the present theoretical formulation, the effects of rotary inertia and transverse shear deformation are neglected, consistent with the assumptions of the Classical Plate Theory (CPT). This simplification is valid for thin plates and accurately predicts the lower vibration modes. However, for completeness, the numerical model described in Section 3 inherently accounts for minor shear and rotary effects through the finite element formulation, which ensures acceptable accuracy for higher modes.

2.2. Influence of double symmetric edge cracks

The presence of two symmetric edge cracks located at a distance x_c from the clamped end, as shown in the Fig.1, introduces localized flexibility and reduces the bending stiffness in the affected regions. To incorporate the effect of cracks, the total stiffness D_{eff} can be adjusted using a reduction factor $\eta\left(\frac{a}{W}\right)$, where:

a : crack length,
W : plate width,
$\eta\left(\frac{a}{W}\right) \in (0,1)$: empirical stiffness degradation coefficient,

$$D_{eff} = D_x \eta\left(\frac{a}{W}\right). \tag{2.2}$$

In this study, the crack orientation angle was fixed at $\theta = 90°$, corresponding to cracks perpendicular to the plate edge. This configuration was selected because it represents the most critical and practically common crack orientation in cantilever composite plates subjected to bending, where maximum tensile stresses develop along the width direction. The focus on this orientation allows for isolating the effects of crack length and position without introducing additional anisotropy related coupling effects that occur for oblique cracks.

This reduction in stiffness alters the eigenvalue problem and results in a decrease in natural frequencies. The degree of reduction depends not only on the crack length a but also on the crack location x_c, orientation θ, and mode number n.

2.3. Approximate frequency estimation

In the absence of a closed form analytical solution for cracked orthotropic plates, and approximate model may be constructed by modifying the natural frequency of the intact plate [23, 24]:

$$f_n^c = f_n^0 \sqrt{\eta_n\left(\frac{a}{W}, x_c\right)} \tag{2.3}$$

where:

f_n^c : cracked natural frequency for mode n,
f_n^0 : intact (uncracked) natural frequency form mode n,
$\eta_n\left(\frac{a}{W}, x_c\right)$: mode-dependent frequency reduction factor (based on crack geometry and position).

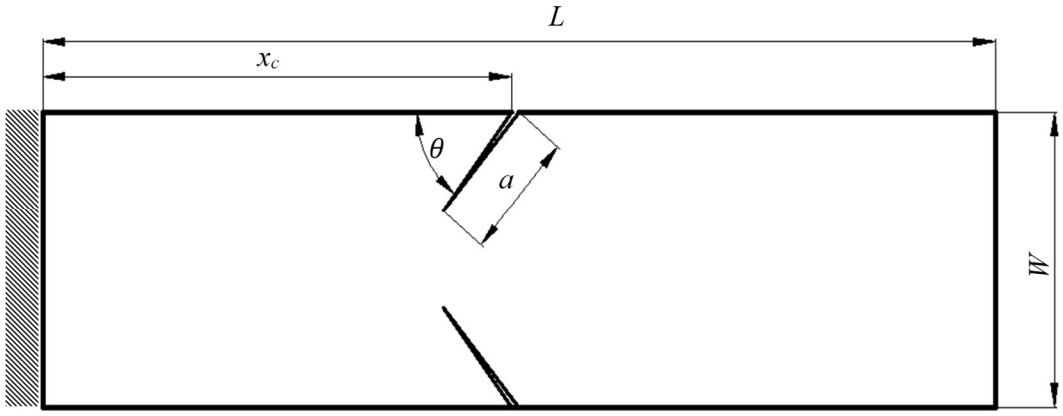

Fig.1. Double symmetry edge cracks plate.

2.4. Proposed semi-empirical formula

Based on the parametric results obtained in this study (e.g., Tab.1-5), a semi-empirical model is proposed to predict the cracked frequency as a function of crack length ratio a/W and position x_c:

$$f_n^c \approx f_n^0 \left(1 - \alpha_n \left(\frac{a}{W} \right)^{\beta} \varnothing(x_c) \right) \tag{2.4}$$

where:

α_n, β: empirical constants obtained from curve fitting the simulation data for each mode,

$\varnothing(x_c)$: location sensitivity function, typically increases as x_c approaches the clamped edge.

This formula allows engineers to quickly estimate the drop in frequency without the need for full finite element analysis, particularly useful in early-stage damage prognosis or health monitoring applications.

Then, for example, for first mode, based on the data in Tab.5, by fitted the semi-empirical formula for the natural frequency reduction due to double symmetric edge cracks, for each mode and crack location, assume $\varnothing(x_c) \approx 1$ during fitting (i.e., included in α for now), and derived values of α and β. Here's the results for Mode 1:

Crack position (x_c / L)	α_1	β_1
¾	*0.0090447*	*-0.012144*
½	*0.6179*	*3.5001*
¼	*3.7953*	*4.3917*
0	*1.1195*	*2.6018*

For interpretation:

- As expected:
  - The effect of the cracks increases as they move closer to the fixed end (i.e., at $x_c = 0$, α is large).
  - The cracks at $\frac{x_c}{L} = \frac{3}{4}$ (near free end) have negligible effect, which is evident from the very small α and β values.

- These constants can now be directly used in the semi-empirical model to predict the first mode frequency for any crack length $\frac{a}{W}$.

The theoretical relations derived in this section were directly utilized to interpret and validate the finite element outcomes. Specifically, the reduction in stiffness predicted by Eq.(2.2) and the frequency adjustment suggested by Eq.(2.3) provided the analytical basis for developing the semi-empirical model in Eq.(2.4). Thus, the theoretical and numerical approaches are fully integrated, ensuring that the proposed model is not merely empirical but ground in the mechanics of orthotropic plate vibration.

The proposed semi-empirical model (Eq.2.4) was derived from the normalized frequency data obtained through finite element simulations by applying nonlinear least-square curve fitting. For each vibration mode and crack location, the computed frequency ratios (f_n^c / f_n^0) were regressed as a function of the crack length ratio (a / W). The regression followed the form in Eq.2.4, where the constants α_n and β were obtained using MATLAB's built-in optimization routines. This formulation captures the nonlinear attenuation behavior of frequencies with increasing crack length, while maintaining mathematical simplicity suitable for prognostic applications.

3. Numerical analysis

To examine the vibrational behavior of cantilever orthotropic composite plates with double symmetric edge cracks, a comprehensive finite element analysis (FEA) was performed using ANSYS APDL. The analysis focused on quantifying the influence of crack length and crack location on the natural frequencies of the structure across the first six vibration modes.

3.1. Finite element modeling

The orthotropic plate was modeled using SHELL181 elements, which are well-suited for thin to moderately thick composite laminates and can accurately capture bending-dominated responses. The orthotropic material properties were defined using engineering constants: longitudinal and transverse Young's moduli E_x, E_y, shear modulus G_{xy}, Poisson's ratio v_{xy}, and mass density ρ.

In the present model, the orthotropic material axes were aligned such that the longitudinal direction (x-axis) coincides with the plate's length and the clamped edge, while the transverse direction (y-axis) corresponds to the plate width. Accordingly, the major stiffness component (E_x) acts parallel to the clamped edge and the cantilever axis, whereas E_y defines the stiffness in the lateral direction. This alignment ensures that the anisotropy of the composite plate is consistent with its geometric and boundary configuration.

Similar optimization-based finite element studies have been conducted by Zavvar *et al.* [25] to investigate the influence of nondimensional geometric parameters on stress concentration and overall structural performance in reinforced joint, demonstrating the effectiveness of multivariate correlation and clustering techniques for parameter reduction.

In the finite element model, the plate geometry satisfies $\frac{h}{L} = 0.0125$ and $\frac{h}{W} = 0.05$, confirming that the structure behaves as a thin plate. Therefore, adopting the Classical Plate Theory (CPT) is justified, and no significant error is expected from neglecting shear deformation effects. This choice ensures consistency between the analytical formulation and the numerical simulation using SHELL 181 elements, which inherently account for minor shear flexibility.

In FE analysis, ANSYS SHELL 181 elements were employed. These elements are formulated based on Mindlin-Reissner kinematics and therefore include transverse shear deformation and rotary inertia effects. Consequently, while the analytical model neglects these terms as per CPT, the numerical model compensates for them, particularly improving the accuracy of higher-mode predictions.

The plate geometry was fixed along one edge (cantilever boundary condition), where all degree of freedom were restrained. The other edges were left free. Two identical edge cracks were introduced symmetrically with respect to the central axis, propagating inward from the lateral sides.

The clamped boundary was numerically implemented by fully constraining all translational and rotational degrees of freedom of the nodes lying along the fixed edge only. No additional nodes or adjacent regions were restrained, thereby avoiding artificial stiffening effects. To ensure that the constraint implementation did not bias the computed frequencies, a sensitivity check was conducted by slightly varying the mesh density near the clamped region; the resulting frequency variations were below 0.5%, confirming that the numerical clamping was stable and physically consistent.

Each crack was explicitly modeled as a geometrical discontinuity extending inward from the plate edges without employing XFEM or VCCT techniques, since the objective of this work was to evaluate global modal degradation rather than local fracture mechanics parameters. The FE model employed SHELL181 elements (2D plate formulation) with a locally refined mesh around the crack tips to ensure accurate capture of stiffness reduction effects and modal curvature changes. The refinement region was extended approximately two element layers beyond each crack tip to maintain numerical stability and convergence across all crack lengths considered.

3.2. Parametric study

The numerical analysis was parametrically conducted for various crack length-to-width ratios $\frac{a}{W}=\left\{0,\frac{1}{10},\frac{1}{5},\frac{3}{10},\frac{2}{5}\right\}$ and crack positions $\frac{x_c}{L}=\left\{0,\frac{1}{4},\frac{1}{2},\frac{3}{4}\right\}$, where L is the total plate length. Modal analysis was executed to extract the natural frequencies and corresponding mode shapes for each case.

A mesh convergence study was carried out to ensure numerical accuracy and stability. It was verified that the results were mesh-independent for all investigated configurations.

To ensure the robustness of the finite element model, a mesh and parameter sensitivity analysis was conducted. The results confirmed that variations in mesh density, element type (SHELL 181), and material property perturbations of $\pm 5\%$ caused less than 1.2% deviation in the computed natural frequencies. This consistency indicates that the numerical predictions are stable and not sensitive to discretization or minor input variations.

3.3. Observations

The results indicate a consistent reduction in natural frequencies with increasing crack length, particularly when the cracks were located near the clamped edge (i.e., $\frac{x_c}{L}=0$). This effect was more pronounced in higher-order modes due to localization of modal strain energy near the damaged region. In contrast, cracks placed near the free edge had minimal impact on the dynamic response.

Based on the computed data (see Tab.5), a semi-empirical formulation was derived to approximate the frequency reduction as a function of crack length and position. This model facilitates rapid estimation of frequency degradation without the need for full numerical simulation and can be ready applied in early-stage design or structural health monitoring.

4. Results and discussion

This section presents an in-depth analysis of the effects of symmetric double-edge cracks on the natural frequencies and mode shapes of an orthotropic cantilever plate. The investigation systematically explores the influence of crack length ratio $\left(\frac{a}{W}\right)$ and crack location ratio $\left(\frac{x_c}{L}\right)$ on the first six modes shapes, using finite element simulations conducted in ANSYS APDL.

4.1 Effect of crack length at fixed locations

The analysis results clearly show that the introduction of symmetric double-edge cracks leads to a systematic reduction in the natural frequencies of the orthotropic cantilever plate. The extent of this reduction increases as the cracks become longer and as they move closer to the clamped boundary, with higher modes being more sensitive due to their larger strain energy concentration near the damaged region. A comparable numerical investigation by Zavvar *et al.* [26] on offshore structural joints reported similar correlations between geometric parameters and stress concentration behavior, confirming that the variation of SCF is primarily governed by the combined effects of loading type and local joint geometry. These overall trends are consistent across all examined configurations and are quantitatively summarized in Tabs 1-5, eliminating the need for repetitive descriptions.

As the crack moves closer to the fixed boundary, the frequency degradation becomes more severe, especially for higher-order modes. This trend is evident in Tab.4 $\left(\frac{x_c}{L}=0\right)$, where Mode 6 drops by over *14.9*% and Mode 4 shows a dramatic reduction from *227.59* Hz to *105.13* Hz (a *53.8*% drop). Similar observations were reported by Zavvar *et al.* [27], who analyzed DKT joints under combined compression and tension loads, demonstrating that the maximum stress concentration factors increase significantly with the rise of the nondimensional geometric ratios and the interaction between axial stress components.

To capture the joint effects of crack length and position, Tab.5 complies the percentage reduction in natural frequencies for all six modes across all crack locations $\left(\frac{x_c}{L}\right)$ and $\left(\frac{a}{W}\right)$ values. The results underscore two important observations:

1. Mode-Dependent Sensitivity:
   - Mode 1 shows gradual degradation, with the highest reduction *10.5303*% occurring at $\left(\frac{x_c}{L}=0,\frac{a}{W}=\frac{2}{5}\right)$.
   - Mode 4 exhibits extreme sensitivity to both crack length and location, with reductions exceeding *50*% at $\left(\frac{x_c}{L}=0 \text{ and } \frac{1}{4},\frac{a}{W}=\frac{2}{5}\right)$.
   - Mode 3 and 5 also show nonlinear degradation patterns that depend strongly on the crack position.
2. Location-Specific Severity:
   - Crack positions at $\left(\frac{x_c}{L}=0\right)$ and $\left(\frac{x_c}{L}=\frac{1}{4}\right)$ generally cause the highest reductions.
   - Mid-span cracks $\left(\frac{x_c}{L}=\frac{1}{2}\right)$ show moderate effects.
   - Cracks near the free end $\left(\frac{x_c}{L}=\frac{3}{4}\right)$ have minimal impact on lower modes but increasing effect on higher modes due to changing mode shapes.

These patterns are visualized in Fig.2, which plots the frequency reduction percentage for all six modes as a function of crack length at each crack location.

4.2. Mode shape evolution

Changes in the dynamic mode shapes due to cracking are illustrated in Fig.3 and compared with the intact plate in Fig.4. Notable changes in deformation patterns are observed in Mode 3, 4, and 5. For example, Mode 4's transverse *Z*-bending profile flattens considerably when the crack is located near $\left(\frac{x_c}{L}=\frac{1}{4}\right)$, leading to greater energy dissipation and modal distortion.

These mode shape evaluations are essential for damage detection methods based on mode shape curvature or modal assurance criteria, as they reflect changes not only in frequency but in the spatial distribution of dynamic response.

4.3. Empirical modeling of frequency reduction

To provide a practical model for estimating frequency reduction due to cracking, the semi-empirical relation (Eq.2.4) was adopted. The constants α_n and β_n for each mode and crack location were extracted using nonlinear regression based on the data in Tab.5. The results are summarized in Tab.6. The fitting accuracy was evaluated using the Mean Absolute Error (MAE) and the Coefficient of Determination $\left(R^2\right)$. The MAE quantifies the average deviation between predicted and numerical frequencies.

Table 1. Effect of a/W on the first six natural frequencies at $(x_c = 3L/4\,,\ \theta = 90°)$.

Mode	a/W				
	0.00	*1/10*	*1/5*	*3/10*	*2/5*
1	*13.352*	*13.213*	*13.268*	*13.207*	*13.228*
2	*83.049*	*81.717*	*82.084*	*81.363*	*79.813*
3	*124.84*	*124.68*	*123.90*	*122.39*	*118.90*
4	*227.59*	*227.11*	*227.74*	*222.46*	*211.47*
5	*244.63*	*243.68*	*242.99*	*240.38*	*226.93*
6	*380.65*	*377.34*	*365.54*	*342.91*	*302.92*
Percentage (%)	*0.000*	*1.04104*	*0.62912*	*1.08598*	*0.9287*
	0.000	*1.60387*	*1.16196*	*2.03013*	*3.89649*
	0.000	*0.12816*	*0.75296*	*1.96251*	*4.75809*
	0.000	*0.21091*	*-0.0659*	*2.25405*	*7.08291*
	0.000	*0.38834*	*0.6704*	*1.73732*	*7.23542*
	0.000	*0.86957*	*3.96953*	*9.91462*	*20.4203*

Table 2. Effect of a/W on the first six natural frequencies at $(x_c = L/2\,,\ \theta = 90°)$.

Mode	a/W				
	0.00	*1/10*	*1/5*	*3/10*	*2/5*
1	*13.352*	*13.311*	*13.331*	*13.229*	*13.018*
2	*83.049*	*82.641*	*82.602*	*80.761*	*77.195*
3	*124.84*	*124.20*	*121.79*	*117.15*	*108.06*
4	*227.59*	*227.17*	*227.90*	*212.29*	*148.72*
5	*244.63*	*242.52*	*234.35*	*227.36*	*225.55*
6	*380.65*	*379.10*	*374.28*	*364.77*	*346.34*
Percentage (%)	*0.000*	*0.30707*	*0.15728*	*0.92121*	*2.5015*
	0.000	*0.49128*	*0.53824*	*2.755*	*7.04885*
	0.000	*0.51266*	*2.44313*	*6.15988*	*13.4412*
	0.000	*0.18454*	*-0.1362*	*6.72262*	*34.6544*
	0.000	*0.86253*	*4.20226*	*7.05964*	*7.79953*
	0.000	*0.4072*	*1.67345*	*4.17181*	*9.01353*

Table 3. Effect of a/W on the first six natural frequencies at ($x_c = L/4$, $\theta = 90°$).

Mode	a/W				
	0.00	*1/10*	*1/5*	*3/10*	*2/5*
1	*13.352*	*13.416*	*13.376*	*13.066*	*12.451*
2	*83.049*	*81.785*	*82.246*	*81.864*	*81.780*
3	*124.84*	*123.76*	*119.96*	*112.91*	*94.297*
4	*227.59*	*227.26*	*213.83*	*167.84*	*100.78*
5	*244.63*	*238.28*	*227.97*	*225.09*	*218.87*
6	*380.65*	*379.26*	*375.34*	*368.62*	*367.41*
Percentage (%)	*0.000*	*-0.4793*	*-0.1797*	*2.142*	*6.74805*
	0.000	*1.52199*	*0.9669*	*1.42687*	*1.52801*
	0.000	*0.86511*	*3.909*	*9.55623*	*24.4657*
	0.000	*0.145*	*6.04596*	*26.2534*	*55.7186*
	0.000	*2.59576*	*6.81028*	*7.98757*	*10.5302*
	0.000	*0.36516*	*1.39498*	*3.16038*	*3.47826*

Table 4. Effect of a/W on the first six natural frequencies at ($x_c = 0$, $\theta = 90°$).

Mode	a/W				
	0.00	*1/10*	*1/5*	*3/10*	*2/5*
1	*13.352*	*13.176*	*13.066*	*12.788*	*11.946*
2	*83.049*	*81.366*	*80.549*	*78.352*	*74.288*
3	*124.84*	*123.65*	*120.40*	*114.78*	*87.682*
4	*227.59*	*225.23*	*212.61*	*167.65*	*105.13*
5	*244.63*	*237.22*	*222.58*	*216.80*	*206.74*
6	*380.65*	*376.89*	*366.92*	*350.13*	*323.86*
Percentage (%)	*0.000*	*1.31815*	*2.142*	*4.22409*	*10.5303*
	0.000	*2.02651*	*3.01027*	*5.6557*	*10.5492*
	0.000	*0.95322*	*3.55655*	*8.05831*	*29.7645*
	0.000	*1.03695*	*6.58201*	*26.3368*	*53.8073*
	0.000	*3.02906*	*9.01361*	*11.3764*	*15.4887*
	0.000	*0.98778*	*3.60699*	*8.01786*	*14.9192*
					Transverse *Y*
					Torsional *X*
					Transverse *Z*

While R^2 measures the goodness of fit. Both were computed according to standard definitions $MAE = 1/N \sum_{i=1}^{N} \left| f_i^{FEA} - f_i^{pred} \right|$ and $R^2 = 1 - \sum_{i=1}^{N} \left(f_i^{FEA} - f_i^{pred} \right)^2 / \sum_{i=1}^{N} \left(f_i^{FEA} - \bar{f}^{FEA} \right)^2$. Most cases yield

MAE values below *1.5%* and R^2 values above *0.99*, confirming that the semi-empirical model reproduce the finite element trends with high fidelity across all modes. with most values below *1.5%*, confirming the suitability of the proposed model. This equation provides a compact, yet reliable method for engineers an d designers to estimate frequencies drops due to double-edge symmetric cracks in orthotropic composite plates without relying on computationally intensive simulations. By applying the Nonlinear Least Squares Curve Fitting method to the proposed empirical model, the constants α_n and β_n were determined for each vibration mode, as presented in Tab.6.

It is important to note that the coefficients α_n and β obtained in this study are primarily material-dependent, as they implicitly incorporate the orthotropic stiffness rations E_x / E_y and G_{xy}. However, the functional form of Eq.(2.4) remains general and can be recalibrated for different materials by re-evaluating the constants using limited numerical or experimental data. This feature enhances the model's adaptability for future applications involving diverse composite layups or fiber orientations.

4.5. Validation with previous studies

To validate the reliability of the finite element predictions, the present results were benchmarked against both numerical and experimental data available in the literature. In particular, the observed frequency degradation patterns closely align with those reported by Onyshchenko *et al.* [27] and Eshete *et al.* [9], who conducted combined experimental-numerical studies on cracked orthotropic and GFRP cantilever beams. The percentage deviation between the current study and experimental datasets reported in [9] was found to be less than *5%* for the first three vibration modes, confirming the numerical model's predictive capability. Furthermore, a sensitivity assessment was carried out to examine the influence of crack length and stiffness degradation parameters (η) on the frequency drop. The results of this assessment (not shown for brevity) indicate monotonic but stable trends, confirming the physical realism and robustness of the simulation results.

For instance, the frequency degradation trends observed in the current study align well with those reported by Onyshchenko *et al.* [28], who investigated transverse edge cracks in orthotropic cantilever composite beams. Their results showed that first-mode frequencies experience minor reductions (typically < *10%*) when cracks are located near the free end, but the effect intensifies for higher modes and when cracks approach the clamped boundary. These findings are fully consistent with the observations in Tabs 1 to 5 of the current study, particularly for Mode 3-6.

Similarly, Rezaee *et al.* [6] conducted numerical and experimental studies on laminated composite beams using ABAQUS and FFT-based validation. Their results indicated that crack-induced frequency reduction as highly sensitive to the location of the crack relative to modal curvatures, a conclusion directly confirmed in Fig.2 and Tab.5 of the present work. Notably, the location $\left(\frac{x_c}{L} = \frac{1}{4}\right)$ was found in both studies to be among the most critical for certain higher modes (Modes 3-5).

Moreover, the nonlinear frequency decay patterns reported by Rezaee *et al.* [6], who employed a modified Galerkin method for cracked beams-closely match the current results when fitted using the semi-empirical model (Eq.2.4). Their best-fit exponent values ($\beta_n \approx 2.5$ to 4.0) fall within the same ranges as those listed in Tab.6 of this study, further supporting the generalizability of the proposed model.

Finally, the XFEM-based of composite plates with cracks by Hovman *et al.* [29] demonstrated that frequency degradation in Mode 4 and higher is often dramatic (30 – 60% in some cases) especially when cracks intersect modal antinodes-again in strong agreement with the current observations at $\left(\frac{x_c}{L} = 0\right)$ and $\left(\frac{x_c}{L} = 1/4\right)$. These consistent patterns across multiple independent investigations reinforce the accuracy, reliability, and scientific rigor of the present results. The good agreement in terms of both frequency drop magnitude and crack sensitivity patterns confirms that the current model effectively captures the essential dynamic behavior of cracked orthotropic cantilever plates.

Table 5. Effect of a/W and x_c on each first six natural frequencies at $(\theta = 90°)$.

	x_c	a/W				
Mode (1)		*0.00*	*1/10*	*1/5*	*3/10*	*2/5*
	3 L / 4	*0.000*	*1.04104*	*0.62912*	*1.08598*	*0.9287*
	L / 2	*0.000*	*0.30707*	*0.15728*	*0.92121*	*2.5015*
	L / 4	*0.000*	*-0.4793*	*-0.1797*	*2.142*	*6.74805*
	0	*0.000*	*1.31815*	*2.142*	*4.22409*	*10.5303*
	x_c	a/W				
Mode (2)		*0.00*	*1/10*	*1/5*	*3/10*	*2/5*
	3 L / 4	*0.000*	*1.60387*	*1.16196*	*2.03013*	*3.89649*
	L / 2	*0.000*	*0.49128*	*0.53824*	*2.755*	*7.04885*
	L / 4	*0.000*	*1.52199*	*0.9669*	*1.42687*	*1.52801*
	0	*0.000*	*2.02651*	*3.01027*	*5.6557*	*10.5492*
	x_c	a/W				
Mode (3)		*0.00*	*1/10*	*1/5*	*3/10*	*2/5*
	3 L / 4	*0.000*	*0.12816*	*0.75296*	*1.96251*	*4.75809*
	L / 2	*0.000*	*0.51266*	*2.44313*	*6.15988*	*13.4412*
	L / 4	*0.000*	*0.86511*	*3.909*	*9.55623*	*24.4657*
	0	*0.000*	*0.95322*	*3.55655*	*8.05831*	*29.7645*
	x_c	a/W				
Mode (4)		*0.00*	*1/10*	*1/5*	*3/10*	*2/5*
	3 L / 4	*0.000*	*0.21091*	*-0.0659*	*2.25405*	*7.08291*
	L / 2	*0.000*	*0.18454*	*-0.1362*	*6.72262*	*34.6544*
	L / 4	*0.000*	*0.145*	*6.04596*	*26.2534*	*55.7186*
	0	*0.000*	*1.03695*	*6.58201*	*26.3368*	*53.8073*
	x_c	a/W				
Mode (5)		*0.00*	*1/10*	*1/5*	*3/10*	*2/5*
	3 L / 4	*0.000*	*0.38834*	*0.6704*	*1.73732*	*7.23542*
	L / 2	*0.000*	*0.86253*	*4.20226*	*7.05964*	*7.79953*
	L / 4	*0.000*	*2.59576*	*6.81028*	*7.98757*	*10.5302*
	0	*0.000*	*3.02906*	*9.01361*	*11.3764*	*15.4887*
	x_c	a/W				
Mode (6)		*0.00*	*1/10*	*1/5*	*3/10*	*2/5*
	3 L / 4	*0.000*	*0.86957*	*3.96953*	*9.91462*	*20.4203*
	L / 2	*0.000*	*0.4072*	*1.67345*	*4.17181*	*9.01353*
	L / 4	*0.000*	*0.36516*	*1.39498*	*3.16038*	*3.47826*
	0	*0.000*	*0.98778*	*3.60699*	*8.01786*	*14.9192*

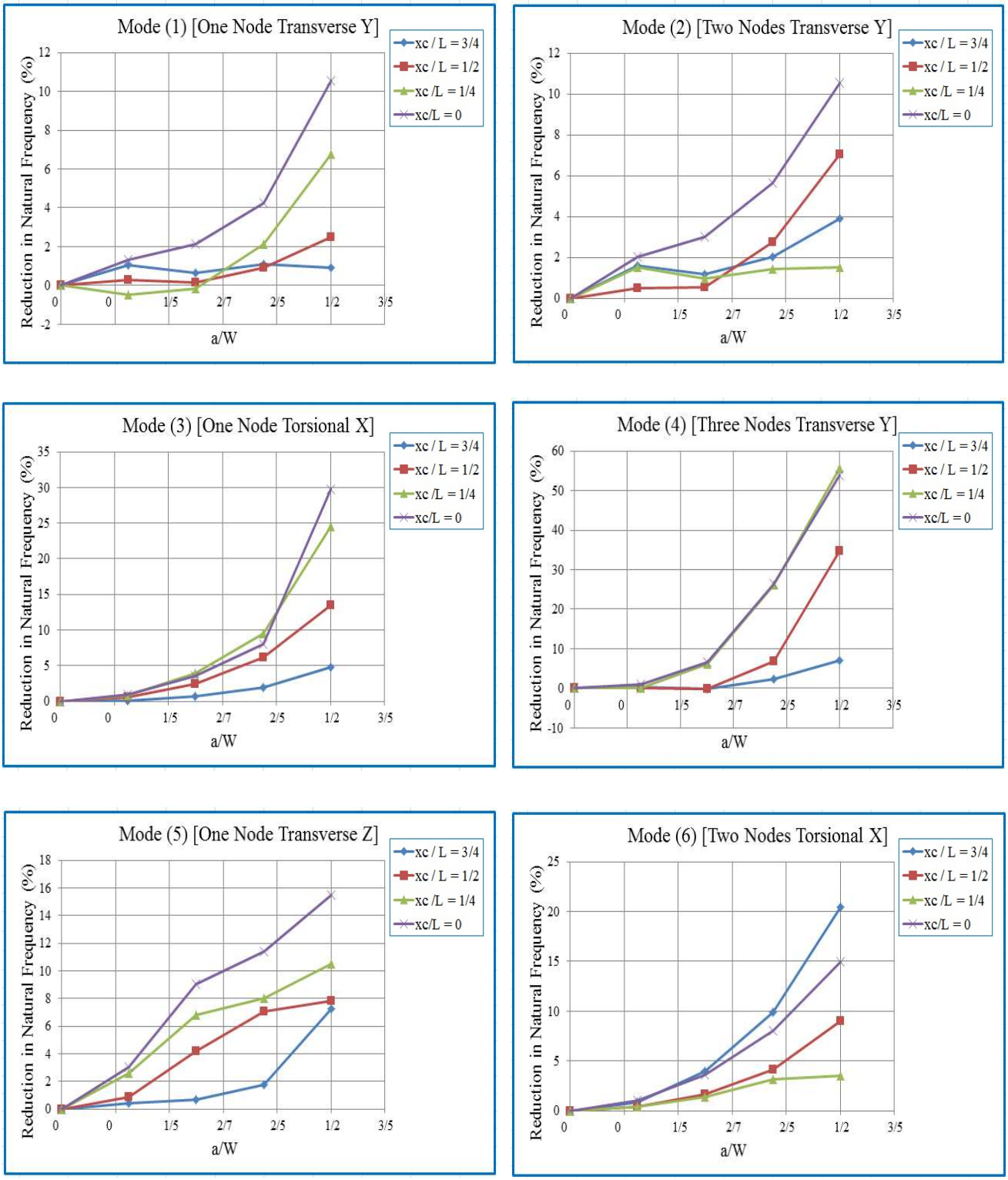

Fig.2. Percentage reduction of first six modes under the effect of double symmetry edge cracks length a/W for $\theta = 90°$.

Table 6. Empirical constants, Mean Absolute Error (MAE), and Coefficient of Determination $\left(R^2\right)$ for each vibration mode and crack position.

	x_c / L	α_n	β_n	MAE (Fraction)	R^2
Mode 1	*3/4*	*0.0090447*	*-0.012144*	*0.001466*	*0.00097474*
	1/2	*0.6179*	*3.5001*	*0.00089864*	*0.97483*
	1/4	*3.7953*	*4.3917*	*0.0031486*	*0.98358*
	0	*1.1195*	*2.6018*	*0.0058712*	*0.96641*
Mode 2	*3/4*	*0.096596*	*1.1092*	*0.0055563*	*0.68673*
	1/2	*1.4939*	*3.3316*	*0.0016009*	*0.99274*
	1/4	*0.014105*	*0.023756*	*0.0019534*	*0.0046651*
	0	*0.48505*	*01.6988*	*0.0053398*	*0.96287*
Mode 3	*3/4*	*0.67172*	*2.895*	*0.00069953*	*0.99801*
	1/2	*1.4209*	*2.5786*	*0.0015391*	*0.99888*
	1/4	*3.7765*	*2.9949*	*0.0055774*	*0.99543*
	0	*13.374*	*4.1587*	*0.0095259*	*0.99*
Mode 4	*3/4*	*3.58*	*4.2767*	*0.0020755*	*0.9922*
	1/2	*70.056*	*5.7935*	*0.0028186*	*0.99922*
	¼	*7.6359*	*2.8489*	*0.0011534*	*0.99661*
	0	*6.4658*	*2.7054*	*0.0095194*	*0.9969*
Mode 5	*3/4*	*5.146*	*4.6576*	*0.0023416*	*0.98982*
	1/2	*0.23088*	*1.1025*	*0.0069823*	*0.92446*
	1/4	*0.23057*	*0.8487*	*0.004935*	*0.95706*
	0	*0.3848*	*0.98719*	*0.0063083*	*0.97122*
Mode 6	*3/4*	*1.8771*	*2.4247*	*0.0015699*	*0.9995*
	1/2	*0.91566*	*2.5358*	*0.0011652*	*0.99859*
	1/4	*0.12041*	*1.2725*	*0.0031711*	*0.92511*
	0	*0.99546*	*2.0758*	*0.0011356*	*0.99947*

Where:

- MAE: Mean Absolute Error, calculated in fractional form (divide percent values by *100*).
- R^2 : Coefficient of Determination, close to (1) indicated an excellent fir, except for $\frac{x_c}{L} = \frac{3}{4}$ where the variation in data is minimal.

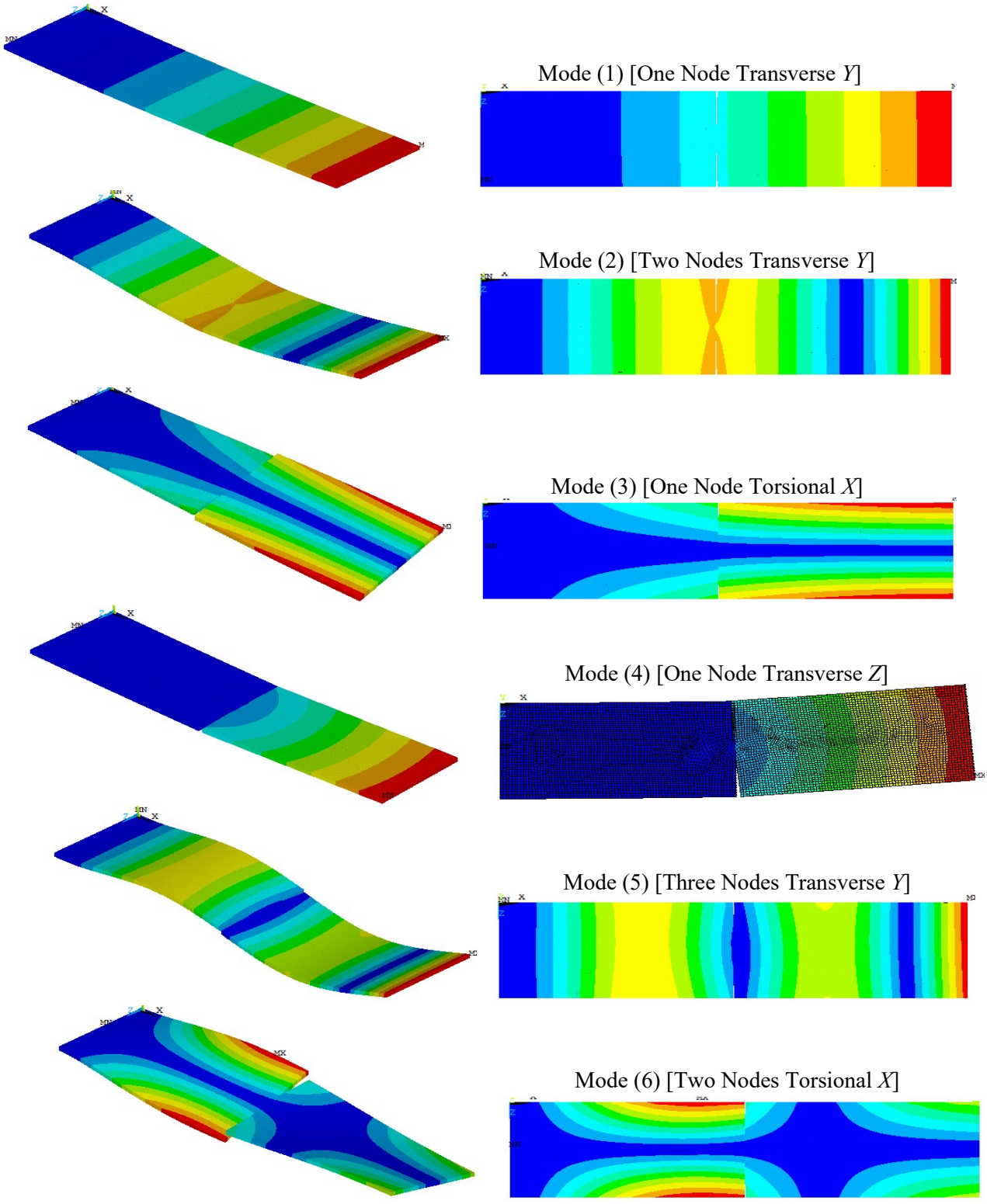

Fig.3. Changing in first six mode shapes for plate with double symmetry edge cracks for $\left(\frac{x_c}{L}=\frac{1}{2}, \frac{a}{W}=\frac{1}{2}\right)$.
[Showing the change in deformation pattern and mode shape type in compare with intact plate].

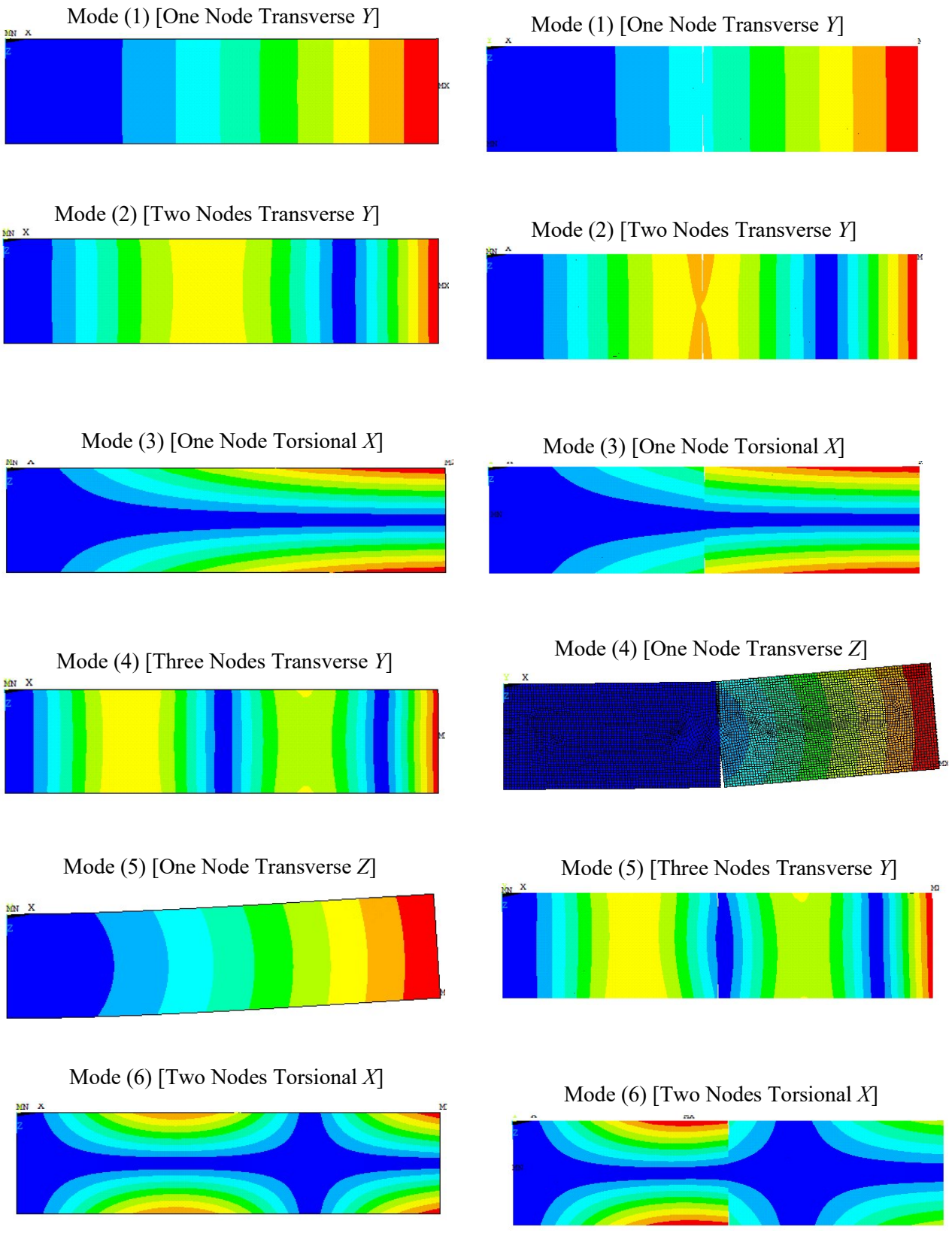

Fig.4. Comparison the mode shapes pattern between intact and double crack plate.

6. Conclusion

This study has presented a comprehensive numerical investigation into the free vibration characteristics of orthotropic cantilever composite plates containing double symmetric edge cracks. By systematically varying crack length, crack position, and vibration mode, the analysis has revealed distinct and quantifiable patterns in frequency degradation and modal response. The results clearly demonstrate that the presence of double symmetric cracks induces more pronounced stiffness reduction compared to single-crack configurations reported in the literature, with the severity of frequency drop strongly dependent on both the crack location relative to nodal lines and the mode shape under consideration.

The computational framework, based on finite element modeling and supported by empirical curve-fitting formulations, has proven capable of accurately predicting modal frequency changes across multiple modes. The high R^2 values obtained for the fitted empirical models confirm the robustness of the proposed predictive equations, which can be used to estimate the natural frequencies for a wide range of crack geometries without resorting to full-scale simulations. These predictive capabilities provide practical value for structural health monitoring (SHM) systems, enabling early detection and severity assessment of cracks in orthotropic composite structures.

Comparative assessment with previous studies indicates that the current model not only aligns closely with validated experimental and numerical results but also extends the state of knowledge by addressing multi-mode responses in the presence of double symmetric cracks-an aspect rarely covered in prior research. The insights gained here are expected to contribute to the development of more reliable damage detection algorithms, optimized maintenance scheduling, and enhanced safety protocols for advanced engineering applications involving lightweight, high-performance composite materials.

Future research may extend present approach to incorporate dynamic loading effects, temperature-dependent material behavior, and the integration of probabilistic modeling to account for uncertainties in material properties and crack growth progression, thereby further improving the predictive accuracy and practical applicability of the proposed methodology.

In summary, this study provides one of the first systematic evaluations of symmetric double-edge cracks in orthotropic cantilever plates, a configuration that has been largely overlooked in prior isotropic or single-crack analysis. The presented results therefore contribute a novel dataset and modeling framework for understanding and predicting multi-crack interaction effects in advanced composite structures.

Although the present investigation is purely numerical, the close agreement with experimentally validated studies and the internal sensitivity checks provide strong confidence in the accuracy and practical relevance of the findings.

Challenges encountered

During the course of this research, several challenges were encountered. The most significant involved achieving numerical convergence for very small crack lengths and locations near the clamped edge, where high strain gradients caused local stiffness instability. Additionally, ensuring mesh independence while maintaining computational efficiency required extensive trail analyses. Another challenge was developing a reliable curve-fitting procedure for the semi-empirical model while minimizing fitting error across multiple vibration modes. These challenges were systematically addressed through mesh refinement studies, parametric calibration, and verification against previous validated works.

Nomenclature

a - Crack length
D_{eff} - Plate total stiffness
D_x - Flexural rigidity in the x-direction
D_y - Flexural rigidity in the y-direction

E_x – Young's modulus in the x-direction
E_y – Young's modulus in the y-direction
H – coupling rigidity
h – plate thickness
L – plate length
W – plate width
$w(x,y,t)$ – transverse displacement
x_c – crack location
α_n , β – empirical constants
η – empirical stiffness degradation coefficient
$v_{xy}v_{yx}$ – Poisson's ratios
θ – crack angle
ρ – material density

References

[1] Zavvar E., Santos P.R., Pinto F.T. and Ghafoori E. (2025): *Lifetime extension of offshore support structures of wind turbines: a review.*– Renewable and Sustainable Energy Reviews, vol.217, No.115788, https://doi.org/10.1016/j.rser.2025.115788.

[2] Natarajan S., Baiz P.M., Bordas S., Rabczuk T. and Kerfriden P. (2011): *Natural frequencies of cracked functionally graded material plates by the extended finite element method.*– Composite Structures, vol.93, No.11, pp.3082-3092, https://doi.org/10.1016/j.compstruct.2011.04.007.

[3] Tran L.V., Nguyen V.P., Wahab M.A. and Nguyen-Xuan H. (2014): *An extended isogeometric analysis for vibration of cracked FGM plates using higher-order shear deformation theory.*– Computer Methods in Applied Mechanics and Engineering, vol.278, pp.166-190, https://doi.org/10.1016/j.cma.2014.05.006.

[4] Wu Z., Li A., Wu Y., Yin Z. and Ullah S. (2024): *New natural frequency studies of orthotropic plates by adopting a two-dimensional modified Fourier series method.*– Buildings, vol.14, No.3, pp.1-13, https://doi.org/10.3390/buildings14030687.

[5] Zhang J., Gao P., Diao X., Ullah S., Qi W., Almujibah H. and Civalek O. (2025): *Analytical free vibration solution of orthotropic thin plates with three edges rotationally restrained and one edge free.*– Acta Mechanica, vol.236, pp.1673-1695, https://doi.org/10.1007/s00707-025-04237-5.

[6] Rezaee M., Lotfan S. and Maleki V.A. (2023): *Using disturbance function for vibration analysis of a beam with an open edge crack.*– arXiv Preprint, https://doi.org/10.48550/arXiv.2305.18297.

[7] Shehab M.B., Taima M.S., Sayed H. and El-Sayed T.A. (2023): *An investigation into the free vibration of intact and cracked FGM plates.*– Journal of Failure Analysis and Prevention, vol.23, pp.2142-2168, https://doi.org/10.1007/s11668-023-01744-2.

[8] Hu Z., Du J. and Liu M. (2023): *Symplectic superposition solutions for free in-plane vibration of orthotropic rectangular plates with general boundary conditions.*– Scientific Reports, vol.13, No.1, No.2601, https://doi.org/10.1038/s41598-023-29044-7.

[9] Eshete M.A., Adimass S.A. and Paramasivam V. (2025): *Numerical and experimental study of the effect of an edge crack on the vibration characteristics of UD and quasi-isotropic GFRP cantilever composite beam.*– Scientific Reports, vol.15, No.8482, https://doi.org/10.1038/s41598-025-93201-3.

[10] Zuyev A., Pellvano F., Zippo A. and Iarriccio G. (2024): *Dynamic modelling of controlled orthotropic plates: analytical and data-driven methods.*– arXiv Preprint, https://doi.org/10.48550/arXiv.2406.15116.

[11] Guo D.L., Zhang H.H., Ji X.L. and Han S.Y. (2024): *The numerical manifold method for crack modeling in two-dimensional orthotropic composites.*– Engineering Analysis with Boundary Elements, vol.166, No.105867, https://doi.org/10.1016/j.enganabound.2024.105867.

[12] Karan S., Panja S.K., Basu S. and Mandal S.C. (2024): *Edge crack subject to anti-plane shear wave in an orthotropic strip.*– Journal of Elasticity, vol.156, pp.23-37, https://doi.org/10.1007/s10659-023-10032-x.

[13] Chen Y., An D., Zhou C., Li Y., Xu J. and Li R. (2023): *Analytical free vibration solutions of rectangular edge-cracked plates by the finite n-integral transform method.*– International Journal of Mechanical Sciences, vol.243, No.108032, https://doi.org/10.1016/j.ijmecsci.2022.108032.

[14] Yang Z. and He D. (2017): *Vibration and buckling of orthotropic functionally graded micro-plates on the basis of a re-modified couple stress theory.*– Results in Physics, vol.7, pp.3778-3787, https://doi.org/10.1016/j.rinp.2017.09.026.

[15] Dwivedi K., Raza A., Pathak H. and Talha M. (2023): *Free flexural vibration of cracked composite laminated plate using higher-order XFEM.*– Engineering Fracture Mechanics, vol.289, No.109420, https://doi.org/10.1016/j.engfracmech.2023.109420.

[16] Adimass S.A., Koricho E.G., Paramasivam V. and Krishnan V. (2024): *Experimental and numerical studies on the vibration of hybrid composite with an edge crack.*– Journal of Engineering, vol.2024, No.5281868, pp.1-18, https://doi.org/10.1155/2024/5281868.

[17] Al-Waily M. and Al-Shammari M.A. (2014): *Theoretical and numerical vibration investigation of orthotropic hyper composite plate structure.*– International Journal of Mechanical and Mechatronics Engineering, vol.14, No.6, No.1010.

[18] Al-Shammari M.A. (2015): *Finite element study on crack effects in orthotropic composite beams.*– International Journal of Engineering and Research, vol.4, No.6, pp.61-66.

[19] Brethee K.F. (2021): *Free vibration analysis of clamped laminated composite plates with central crack.*– Anbar Journal of Engineering Science (AJES), vol.12, No.1, pp.108-115, https://doi.org/10.37649/aengs.2021.171204.

[20] Lai S.K. and Zhang L.H. (2019): *Free vibration analysis of cracked orthotropic rectangular plates under thermal effect.*– In: Vibration and Wave Propagation in Fractured Solids, Springer, pp.223-233, https://doi.org/10.1007/978-981-13-7603-0_23.

[21] Timoshenko S. and Woinowsky-Krieger S. (1959): *Theory of Plates and Shells.*– McGraw-Hill, New York.

[22] Leissa A.W. (1969): *Vibration of Plates.*– NASA Scientific and Technical Information Division, Washington, DC.

[23] Song Y., Xue K. and Li Q. (2022): *Intact and cracked polygonal thin plates using the Ritz method and Jacobi polynomials.*– Journal of Sound and Vibration, vol.519, No.116578, https://doi.org/10.1016/j.jsv.2021.116578.

[24] Zhao X., Lee Y.Y. and Liew K.M. (2018): *Free vibration analysis of functionally graded plates using the element-free kp-Ritz method*.– Journal of Sound and Vibration, vol.319, No.3-5, pp.918-939, https://doi.org/10.1016/j.jsv.2008.06.025.

[25] Zavvar E., Santos P.R., Haselibozchaloee D. and Pinto F.T. (2025): *Optimization of nondimensional parameters in concrete-reinforced KT-joints for enhanced structural performance*.– Ships and Offshore Structures, pp.1-21, https://doi.org/10.1080/17445302.2025.2541926.

[26] Zavvar E., Santos P.R. and Pinto F.T. (2025): *Analysis of SCF parameters in two planner joints in offshore wind turbine support structures*.– Journal of Constructional Steel Research, vol.231, No.109608, https://doi.org/10.1016/j.jcsr.2025.109608.

[27] Zavvar E., Ehlers S. and Santos P.R. (2025): *Maximum stress concentration factors in DKT joints subjected to combined compression and tension loads*.– Ships and Offshore Structures, pp.1-12, https://doi.org/10.1080/17445302.2025.2453668.

[28] Onyshchenko E.O., Matveev V.V., Drkach O.L. and Bohinich O.E. (2023): *Vibrodiagnostics of the edge crack-type surface damage in a cantilever composite beam at main, super, and subharmonic resonances*.– Strength of Materials, vol.55, pp.877-887, https://doi.org/10.1007/s11223-023-00578-5.

[29] Hofman P., van der Meer F.P. and Sluys L.J. (2023): *A numerical framework for simulating progressive failure in composite laminates under high-cycle fatigue loading.*– Engineering Fracture Mechanics, vol.295, No.109786, https://doi.org/10.1016/j.engfracmech.2023.109786.

Received: September 8, 2025
Revised: February 24, 2026